PROCEEDINGS of the
23rd International Congress on Acoustics

9 to 13 September 2019 in Aachen, Germany

Extraction of high contributing sound of Air Handling Unit and noise reduction using transfer path analysis

Takuya HIRAO[1]; Yousuke MIYAMOTO[1]; Junji YOSHIDA[1]

[1] Osaka Institute of Technology, Japan

ABSTRACT

Air handling unit (AHU) is generally built in a machine room of a building and controls the temperature in multiple office spaces. The motors of AHU generate sound and vibration and have a possibility to cause noise problem in office. Accordingly, it is necessary to extract high contributing part of the AHU and apply intensive countermeasures to the part quickly. In this study, we attempted to reduce the noise by applying the operational TPA to the simple AHU model. In the test, the radiated sound in front of the model was recorded and the frequency band which increased the overall noise level was extracted. In addition, operational TPA was applied to find out the main contributor to the radiated noise. As the result, the noise at 200 Hz band was large and the motor radiated noise was found to be the main contributor. Furthermore, the noise was increased in the unit case by the cavity resonance. Then, the inside volume of the AHU was separated using a plastic plate for the reduction of the motor noise in the unit. The result showed that the unit radiated noise at the frequency band could be decreased well.

Keywords: Air handling unit, Radiated noise, Transfer path analysis

1. INTRODUCTION

Air handling unit (AHU) is a system for controlling temperature, humidity and air flow of multiple office spaces (1). This system is generally built in a machine room of the building placed on near office. Hence, the system may cause the noise and vibration problems to the office spaces by transmitting the noise and vibration of the unit. In the noise reduction activity of AHU, finding out the main contributors to the radiated noise and applying intensive countermeasure to the part is essential to realize the effective countermeasure. However, when the noise problem occurs and the people in office recognize it, the unit is already installed and the office is already running. Accordingly, we cannot use adequate duration for the analysis and the countermeasure. In such a case, an instant analytical technique for obtaining the high contributing part is required.

In this study, we attempted to utilize operational transfer path analytical (TPA) method to the original AHU model to realize the effective noise and vibration analysis for AHU. In addition, we actually tried the radiated noise reduction using the analytical results and a fundamental CAE technique to verify the effectivity of the method.

2. NOISE MEASUREMENT OF AIR HANDRING UNIT

In this study, simple AHU model was made to analyze the radiated noise of AHU as shown in Fig. 1 (a). This model was a small size based on a compact AHU system having frame, two fun motors and the air ducts. The length, width and height were 400 x 1600 x 800 mm. Each part and the air flow image are described in Fig. 1 (b).

[1] junji.yoshida@oit.ac.jp

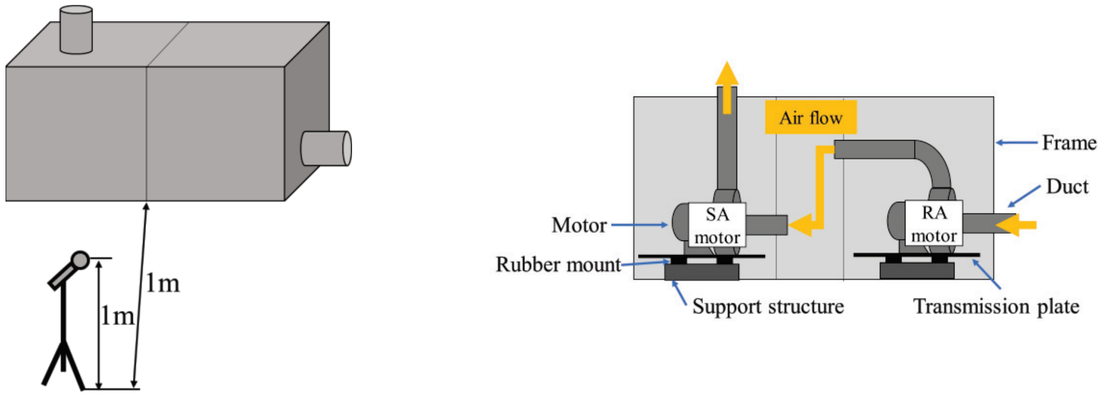

(a) – Outside view (b) – Internal parts and air flow

Figure 1 – Air handling unit model

The radiated noise was recorded at first to grasp the sound characteristics. In the recording, sound pressure signal was measured using a microphone positioned at 1 m from the front of the AHU model at a height of 1 m as shown in Fig. 1 (a). As the AHU condition during the recording, the supply air motor (SA motor) and the return air motor (RA motor) speed were increased from 0 to 3600 rpm for 20 s. After then, the speed was constant at 3600 rpm for 10 s. Figure 2 shows the averaged A-weighted SPL of the radiated noise.

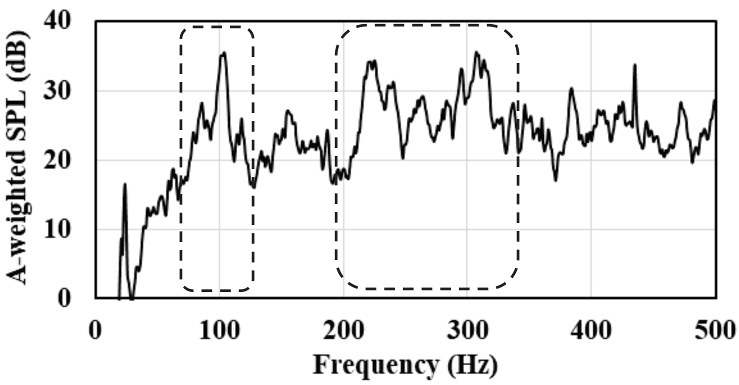

Figure 2 – Averaged spectrum of the radiated noise of AHU

Horizontal and vertical axes show frequency and A-weighted SPL, respectively. From this figure, A-weighted SPL peaks were found at 100 Hz, 200-250 Hz, and 300 Hz bands. These peaks seem to be the main factors deteriorating the quietness of the AHU. Hereafter, we analyze the main contributing parts to the radiated noise at the frequency bands using TPA for the effective countermeasure to improve the quietness of the AHU model.

3. FACTOR ANALYSIS OF NOISE USING OPERATIONAL TPA

3.1 Transfer Path Analysis

In this section, we applied TPA to find out the main contributing parts to the radiated noise of AHU. In many kinds of TPA methods (2-5), we applied operational TPA (OTPA) (4, 5). This TPA method was known to be able to calculate the contributions with smaller man-hour comparing with the other methods. In the OTPA, input force are not required to be measured but reference point vibrations or sound pressures at close to input points and the response point (radiated noise) are necessary to be measured simultaneously. The contributions of the response point from the reference points are calculated as follows.

3.2 Procedure of OTPA (4)

In the OTPA, the individual contributions are calculated by two-step processes. In the first step, the transfer function from the reference point to the response point is calculated using various operational signals measured at the reference and response points. In the second step, each contribution is obtained by multiplying the reference point signal by the calculated transfer function. The transfer function in this method is calculated using a principal component regression method. The calculation procedure is shown in Fig. 3.

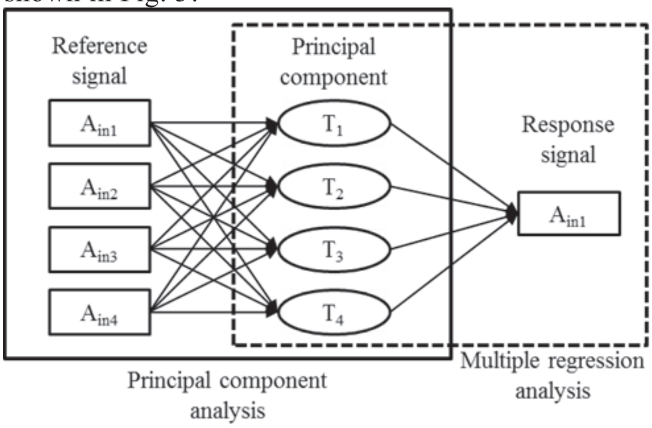

Figure 3 – OTPA model using principal compornent regression method

At first, a response signal and multiple reference signals are transposed to frequency-domain signals from time-domain signals by fast Fourier transform (FFT). The response signal matrix $[A_{out}]$ can be expressed by the reference matrix $[A_{in}]$ and the transfer matrix $[H]$ for each frequency, as follows:

$$[A_{out}] = [A_{in}][H] \quad (1)$$

The (i, j)-th element in the reference matrix $[A_{in}]$ is the data at the j-th reference point in the i-th fast Fourier transform (FFT), and the (i, k)-th element in the response matrix $[A_{out}]$ is the data at the k-th response point in the i-th FFT. The (j, k)-th element in the transfer matrix $[H]$ is the transfer function from the j-th reference point to the k-th response point. Following singular value decomposition (SVD), the reference matrix $[A_{in}]$ can be expressed as follows:

$$[A_{in}] = [U][S][V]^T \quad (2)$$

The principal component (PC) matrix $[T]$ is then obtained using the results of SVD, this procedure is the same as principal component analysis (PCA):

$$[T] = [A_{in}][V] = [U][S] \quad (3)$$

Where $[V]$ is the coefficient matrix for transposing the reference matrix $[A_{in}]$ to the PC matrix $[T]$, and the (i, m)-th element of $[T]$ is the m-th PC in the i-th FFT. Next, multiple regression analysis (MRA) from the PC matrix $[T]$ to the response matrix $[A_{out}]$ was performed, and the regression coefficient matrix $[B]$ was obtained as follows:

$$[A_{out}] = [T][B] \quad (4)$$

$$[B] = ([T]^T[T])^{-1}[T]^T[A_{out}] \quad (5)$$

Where $[B]$ is the coefficient matrix used to transpose the PC matrix $[T]$ to the response matrix $[A_{out}]$, and the (m, k)-th element of $[B]$ is the regression coefficient from the m-th PC to the k-th response point. The transfer function $[H]$ is obtained by multiplying the coefficient matrix $[V]$ with the coefficient matrix $[B]$, as follows:

$$[H] = [V]([T]^T[T])^{-1}[T]^T[A_{out}] \quad (6)$$

$$[H] = [V][S]^{-1}[U]^T[A_{out}] \quad (7)$$

The contribution to the response signal from each reference signal $[A_{out\ cont}]$ can be obtained by multiplying the measured reference signal $[A_{cont}]$ at the contribution separation target condition by the calculated transfer function $[H]$:

$$[A_{out\ cont}] = [A_{in\ cont}][H] \quad (8)$$

The (i, k)-th element in the contribution matrix $[A_{out\ cont}]$ is the contribution at the k-th response point in the i-th FFT. This procedure was used to obtain the contributions in this study.

3.3 Analysis of High Contributing Part to the Radiated Sound

Here, we applied OTPA to find the main contributing parts to the radiated noise. We then used the radiated sound pressure recorded in front of the AHU model as the response signal. As the reference signals, front-back vibration, up-down vibration of SA motor and those of RA motor were employed as shown in Fig. 4. In addition, radiated noise near SA motor and RA motor were also used as the reference signals. These response and reference signals were measured simultaneously to obtain each contribution by OTPA.

As same as the previous test condition, the radiated noise was recorded when the SA motor and RA motor speed was increased from 0 to 3600 rpm for 20 s and the speed was constant at 3600 rpm for 10 s as the operational test condition.

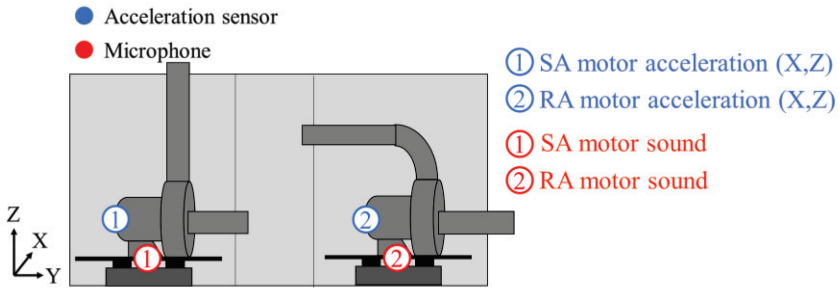

Figure 4 – Measurement points for OTPA

To assess the contribution from each reference signal easily, we calculated group contribution according to the parts position as shown in Fig. 5. In this case, SA motor group contribution and RA motor group contribution were calculated respectively to determine the high contributing part between SA and RA motor. The calculated group contributions are shown in Fig. 6.

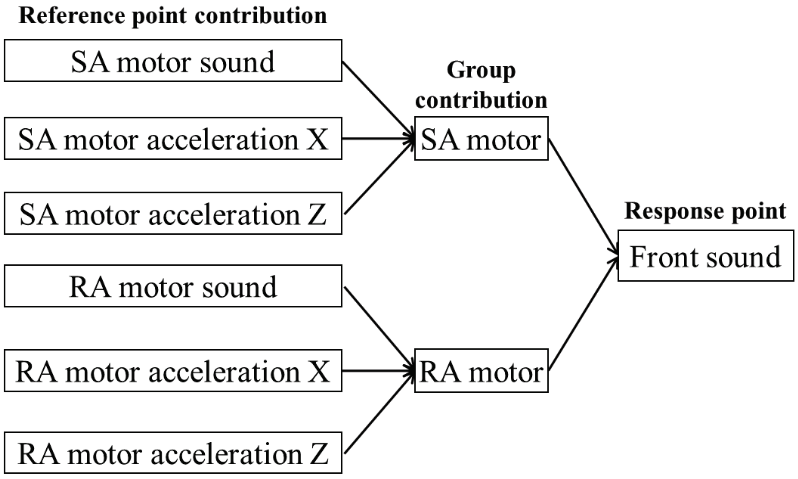

Figure 5 – Contribution of each reference point and group contribution to the response point

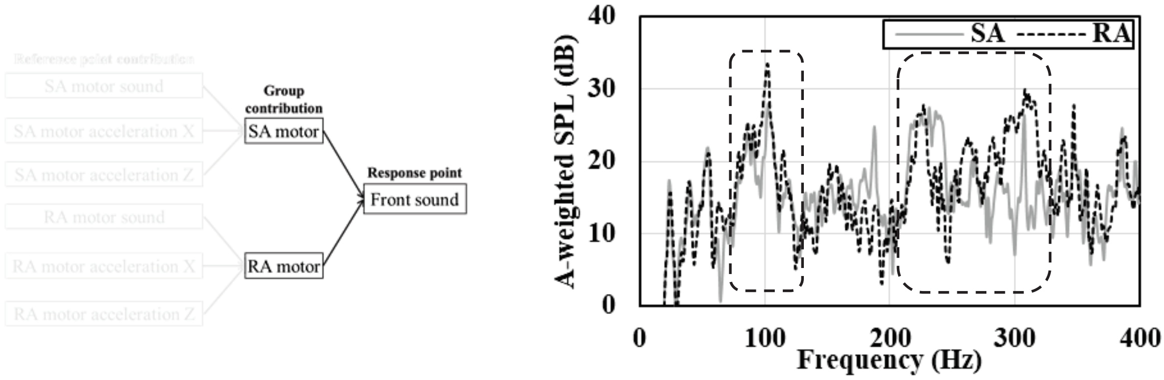

Figure 6 – SA and RA motor contributions

Horizontal and vertical axes of right diagram of Fig. 6 show the frequency and the sound pressure level, respectively. Gray solid and black dotted lines show the SA and RA group contribution. As the result, the RA motor contributions were observed to high at 100 Hz, 200-250 Hz and 300 Hz bands. In addition, the SA motor contributions were also high at 100 and 200-250 Hz bands. Then, each motor sound and acceleration contributions were calculated to obtain the detailed contribution of the motor respectively. The calculated contributions are shown in Fig. 7 and 8.

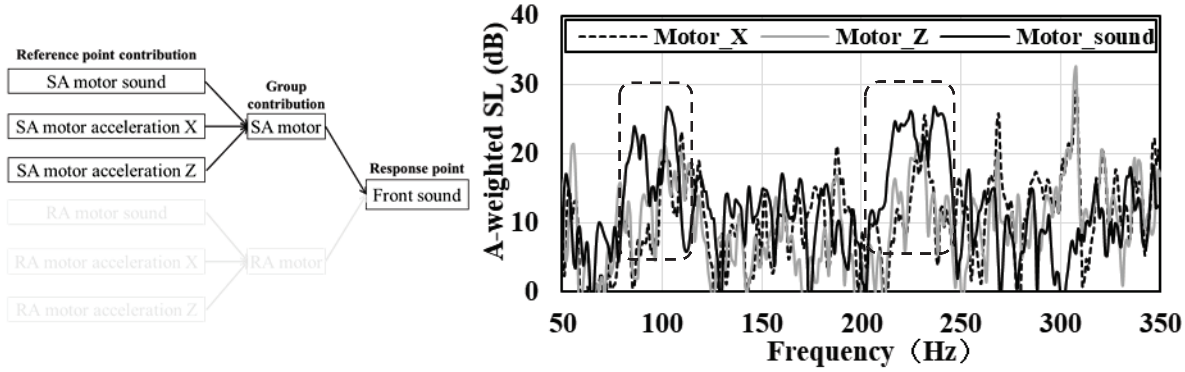

Figure 7 – SA detailed contribution

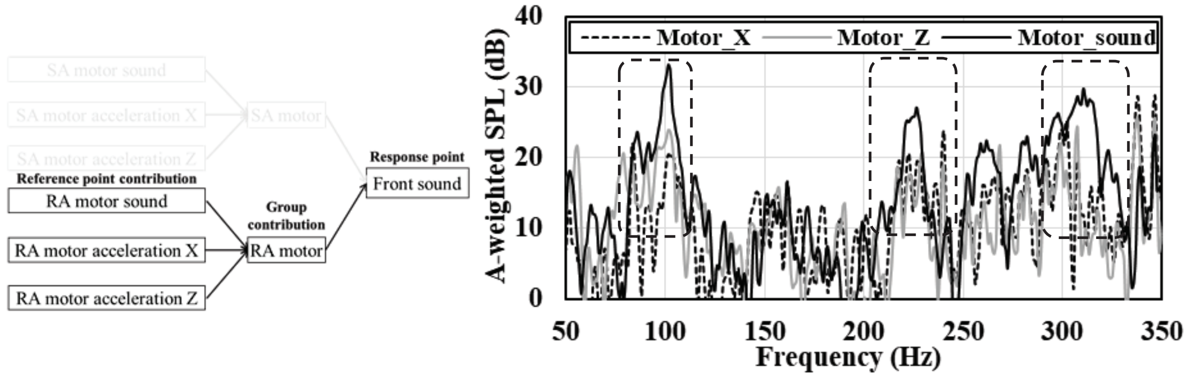

Figure 8 – RA detailed contribution

Figure 7 and 8 show the contribution of motor vibration and sound of SA and RA motors, respectively. From the SA detailed contributions in Fig.7, the SA motor sound contribution was calculated as very high at 100 Hz and 200-250 Hz bands. About the RA detailed contribution in Fig. 8, the motor sound contribution was also high at 100 Hz, 200-250 Hz and 300 Hz bands.

From these results of OTPA, both motor sounds were found to be dominant source to the radiated noise in front of the AHU at 200-250 Hz. Hence, we focused on the frequency band in the following analysis. Figure 9 (a), (b) and (c) shows the SA and RA sound contributions and the sound pressure level and transfer function of SA and RA motor sound which compose the contribution.

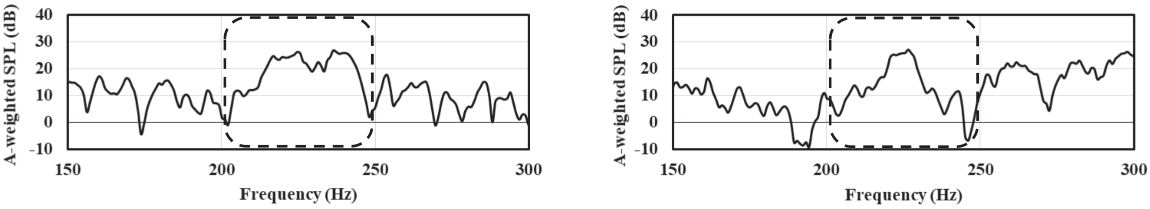

(a) – SA contribution (d) – RA contribution

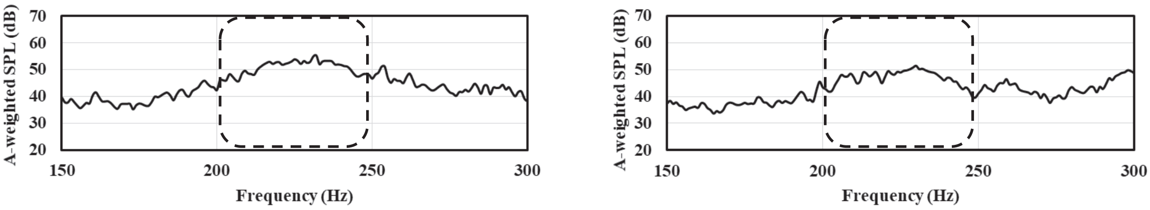

(b) – SA sound pressure signal (e) – RA sound pressure signal

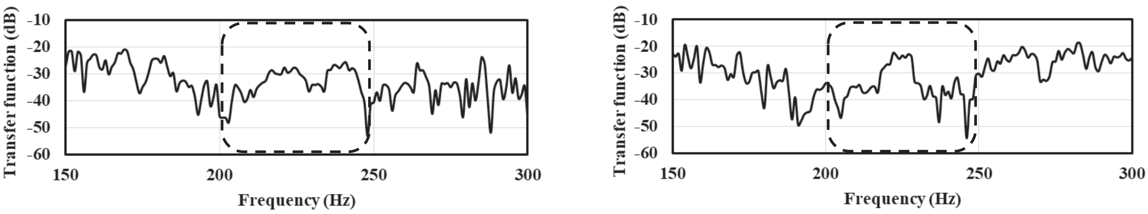

(c) – SA transfer function (f) – RA transfer function

Figure 9 – Contribution, sound pressure signal and transfer function of SA and RA motor

As shown in Fig. 9, the contribution peak at around 200-250 Hz band of SA and RA (Fig. 9 (a) and (d)) were found to be made by the sound pressure signal (Fig. 9 (b), (e)) and the transfer function (Fig. 9 (c), (f)) because both elements had peaks at around the focused frequency. From the results, we supposed that the cavity resonance in the unit case of SA and RA motors increased the sound pressure level near the motors and the transfer functions to the response point.

4. COUNTERMEASURE OF AHU NOISE USING OTPA RESULT

4.1 Eigenvalue Analysis by CAE

In the previous OTPA, we estimated the main factor increasing the front radiated noise at 200-250 Hz band as the resonance in cavity by utilizing the calculated contribution elements. Here, acoustical eigenvalue analysis was carried out to evaluate the estimated factor by using CAE.

Figure 10 shows the acoustical mode of SA cavity at 213 Hz. Noting that the cavity volume and shape of RA was identical of that of SA, hence, the resonance frequency and the acoustical mode became the same.

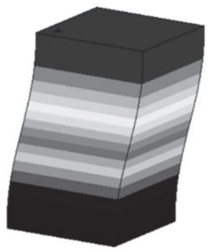

Figure 10 – Acoustical mode of SA and RA cavity at 213 Hz obtained by CAE

As shown in the figure, the acoustic mode along the top-down direction was obtained at 213 Hz in the SA and RA cavity. This frequency met where the SPL and transfer function of SA and RA motors had peak. Hence, the cavity resonance was clarified to be the main factors of the AHU noise peak at 200-250 Hz band.

4.2 Countermeasure

For the reduction of the AHU noise at the target frequency, we then divided the cavity into 2 spaces by using a plastic plate to move the resonance frequency to high as shown in Fig. 11.

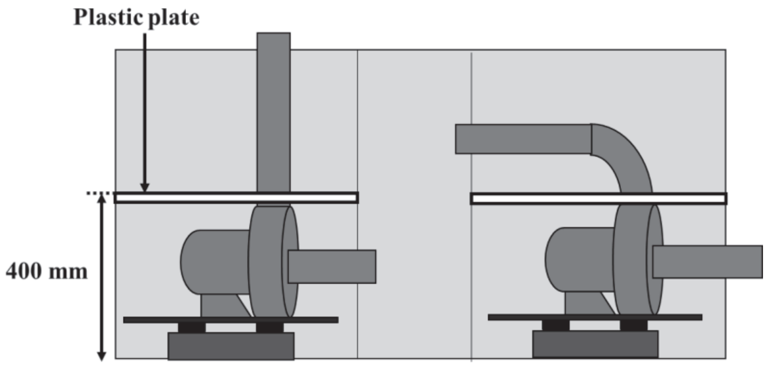

Figure 11 – Modified model by separating the cavity using plastic plate

We again carried out the operational test again before and after the modification to verify the effectiveness of the countermeasure. Figure 12 (a) and (b) shows the comparison of the averaged A-weighted SPL near the SA and RA motor before and after the countermeasure.

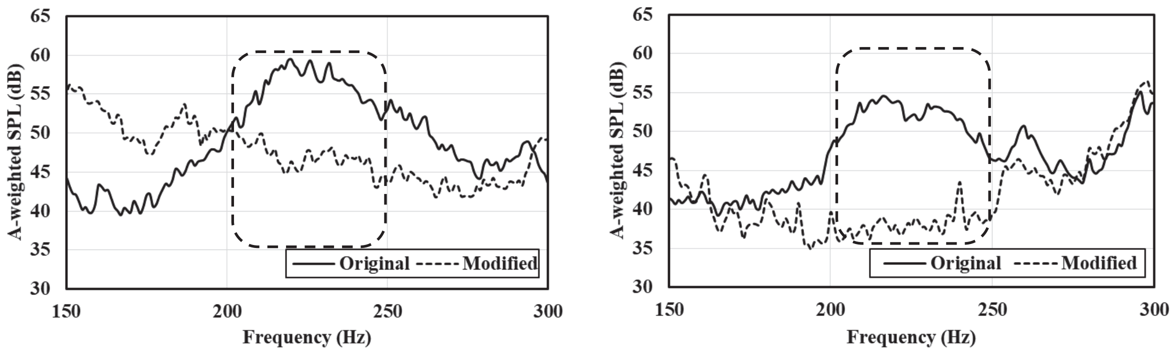

(a) – SA motor SPL (b) – RA motor SPL

Figure 12 – Comparison of SA and RA motor SPL before and after countermeasure

Black solid and dotted lines show the motor sound before and after countermeasure. As shown in these figures, the SPL near SA and RA motors were observed to decrease about 10 dB at the target frequency band. This indicates that the cavity resonance was actually the main factor increasing the SA and RA motor noise at 200-250 Hz.

Then, we recorded the front side SPL of the AHU before and after the modification. Figure 13 shows the comparison of SPL.

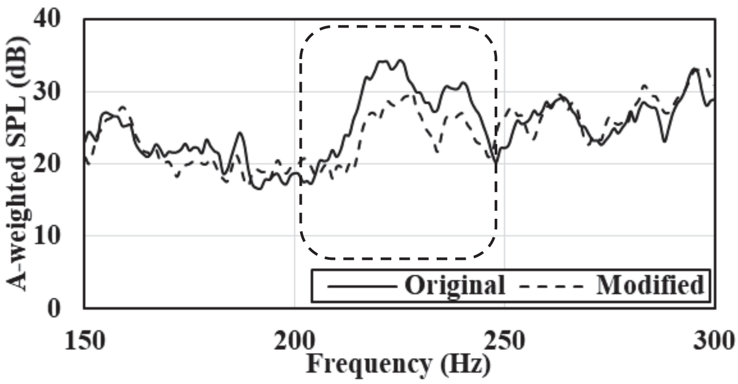

Figure 13 – SPL comparison of the front side radiated noise of AHU

Black solid and gray dotted lines are the averaged SPL of the front side radiated noise of AHU before and after the countermeasure, respectively. As shown in the figure, the SPL only at 200 -250 Hz band could be reduced about 5 dB by taking countermeasure to the cavity resonance estimated by using OTPA and CAE. From these results, the high contributing part to the radiated noise of AHU could be found by applying OTPA and CAE.

5. CONCLUSIONS

In this study, we attempted to utilize an OTPA method to the original AHU model to realize the effective noise reduction of the AHU. In addition, we applied a fundamental CAE technique to evaluate the estimated high contributing part in detail.

Through the radiated noise measurement at the front side of the AHU, the SPL was large at 100 Hz, 200-250 Hz and 300 Hz bands in the operational condition. Then, we applied OTPA to the radiated noise of the AHU model to find out the main contributing parts. As the result, both SA and RA motor sounds and the transfer function to the front side radiated noise of AHU were calculated to have high contribution at 200-250 Hz band. From the analytical results, we estimated the cavity resonance in the unit case of SA and RA motor were the main factors of the AHU SPL peak.

Subsequently, we applied an acoustical eigenvalue analysis to the cavity to consider the main factor of the AHU noise peak at 200-250 Hz in detail. As the result, the cavity resonance frequency was 213 Hz and the acoustical mode in cabin was obtained. Accordingly, we separated the cavity volume by inserting a plastic plate in the SA and RA motor cavity for the verification of the analysis. Consequently, the radiated noise could be decreased about 5 dB only at the target frequency by the countermeasure. This revealed that the method could indicate the correct high contributing part to AHU radiated noise.

From these results, the OTPA and CAE method were clarified to have ability to analysis the important contributing part to the AHU radiated noise for carrying out quick measurement, analysis and countermeasure.

REFERENCES

1. Arizono S., "Function and basic structure of air conditioner AHU (air handling unit) – FCU (fun coil unit)", BE Construction equipment, 2008, p.171.
2. Van der Auweraer H., Wyckaert W., Van Der Linden P., "Noise and Vibration Transfer Path Analysis, Lecture series - van Kareman Institute for fluid dynamics", van Kareman Institute, Rhode-Saint-Genèse, Belgium, 1979.
3. Van der Auweraer H., Mas P., Dom S., Vecchio A., Janssens K., Van de Ponseele P., "Transfer Path Analysis in the Critical Path of Vehicle Refinement: The Role of Fast, Hybrid and Operational Path Analysis", SAE 2007-01-2352, Proceedings SEA Noise and Vibration Conference, St.Charles (IL), USA, 2007, pp.15-17.
4. Noumura K., Yoshida J., "Method of Transfer Path Analysis for Vehicle Interior Sound with No Excitation Experiment", FISITA2006 Proceedings F2006D183, 2006, pp.1-10.
5. Yoshida J., Yoshida S., Okajima M., Hosokawa A., N., Hujii T., "Contribution analysis of drum type washing machine noise during drying using multi-layered operational TPA", Inter Noise17, CHINA, 2017, pp.1195-1204.